Craniometric ratios of microcephaly and LB1, *Homo floresiensis*, using MRI and endocasts

Robert C. Vannucci[a], Todd F. Barron[b], and Ralph L. Holloway[c,1]

[a]Department of Anthropology, New York University, New York, NY 10012; [b]WellSpan Neuroscience, York, PA 17402; and [c]Department of Anthropology, Columbia University, New York, NY 10027

Edited by Richard G. Klein, Stanford University, Stanford, CA, and approved July 12, 2011 (received for review April 7, 2011)

The designation of *Homo floresiensis* as a new species derived from an ancient population is controversial, because the type specimen, LB1, might represent a pathological microcephalic modern *Homo sapiens*. Accordingly, two specific craniometric ratios (relative frontal breadth and cerebellar protrusion) were ascertained in 21 microcephalic infants and children by using MRI. Data on 118 age-equivalent control (normocephalic) subjects were collected for comparative purposes. In addition, the same craniometric ratios were determined on the endocasts of 10 microcephalic individuals, 79 normal controls (anatomically modern humans), and 17 *Homo erectus* specimens. These ratios were then compared with those of two LB1 endocasts. The findings showed that the calculated cerebral/cerebellar ratios of the LB1 endocast [Falk D, et al. (2007) *Proc Natl Acad Sci USA* 104:2513–2518] fall outside the range of living normocephalic individuals. The ratios derived from two LB1 endocasts also fall largely outside the range of modern normal human and *H. erectus* endocasts and within the range of microcephalic endocasts. The findings support but do not prove the contention that LB1 represents a pathological microcephalic *Homo sapiens* rather than a new species, (i.e., *H. floresiensis*).

In September 2003, a team of archeologists discovered the remains of a hominid in a limestone cave on the Island of Flores, Indonesia (1). The skeletal remains included a nearly complete skull and several postcranial elements of a young adult female (LB1) dated to 18,000 y ago (2). The two most notable features of the individual were a small cranium, reflecting a tiny brain relative to modern humans, and a short stature with disproportionate limbs. Further excavations in 2004 yielded skeletal elements of at least eight other individuals in similar strata as the original skeletal find (3). Based on detailed anthropometric data derived from the remains, the investigators concluded that the early inhabitants of Flores were small-brained and small-bodied descendents of Asian *Homo erectus*/archaic *Homo sapiens* or possibly even earlier hominids (i.e., *Australopithecus*). Pursuant to the original description of the specimens, there has been a heated argument as to whether LB1 and her kin represent a truly ancient hominid population that survived a very long time or a modern *H. sapiens* population, one or more of whom suffered pathological microcephaly (4–6).

Collaborating with Brown, Morwood, and others, Falk et al. (5) constructed 3D computed tomographic (CT) endocasts of LB1 along with nine microcephalic and 10 normal *H. sapiens*. Their study was designed to answer the question as to whether LB1 was a small-bodied and small-brained normal individual or a small-bodied individual with a pathologically small brain (i.e., a microcephalic). Having constructed virtual endocasts from the CT images, Falk et al. (5) obtained eight measurements to generate four ratios for comparative purposes. The two variables that provided the most discrimination (100% success) between the microcephalic and normal endocasts were "cerebellar protrusion" and "relative frontal breadth." Specifically, the microcephalic specimens exhibited greater caudal cerebellar protrusion and smaller frontal breadths. LB1's ratios were consistent with the normal endocasts with >99% likelihood. From their analysis, Falk et al. (5) concluded that LB1 was not a pathological microcephalic. Rather, her small brain size and other cranial and postcranial features warranted a species designation other than *H. sapiens* (i.e., *Homo floresiensis*).

However, it must be emphasized that the control data of the Falk et al. (5) investigation included only 10 normocephalic endocasts from a variety of sources as well as nine widely distributed microcephalics. We recently obtained craniometric measurements on much larger normocephalic and microcephalic cohorts by using both MRI and endocasts to determine the relationships of these samples to those of LB1, using the same discriminating ratios as reported by Falk et al. (5).

Results

In their 2007 article, Falk et al. (5) used four craniometric ratios to distinguish the endocasts of microcephalic and normocephalic individuals. All four ratios combined a cerebellar and a cerebral dimension (linear measure) on the assumption that microcephalic brains have smaller cerebral hemispheres relative to their respective cerebellar hemispheres. Two of the four ratios (cerebellar protrusion and relative frontal breadth) were considered highly discriminating. The cerebellar protrusion ratio was obtained by dividing the cerebellar pole—projected frontal pole by the cerebral length. The relative frontal breadth ratio was obtained by dividing the frontal breath (at anterior temporal pole) by the cerebellar width. These two ratios were analyzed in the present MRI dataset. For the analysis of the microcephalic data, normocephalic control brains with ages nearly identical to the individual microcephalic brains were chosen (Table 1). A total of 14/21 microcephalic brains had cerebellar protrusion ratios outside the range of age-matched controls. A total of 6/21 brains had relative frontal breadth ratios outside the range of age-matched controls. Combining the two ratios, 11/21 brains had values outside the control range, 3 of which had individual ratios within their respective control ranges. Totaling the numbers, there were 20/21 brains with individual or combined ratios outside the ranges of age-equivalent normocephalic brains. Accordingly, the two ratios discriminated the microcephalic and normocephalic brains in 95% of the cases.

Having demonstrated that two of the Falk et al. (5) craniometric ratios distinguish living microcephalic from normocephalic individuals, we compared these values to those of LB1. Neither of the ratios for LB1 was cited in any of the Falk et al. articles (5, 7, 8), including online supporting information; but the values were easily extracted from figure 3 of Falk et al. (5) (*Methods*). Cerebellar protrusion of LB1 is 0.965, whereas relative frontal breadth is 1.04, the latter ratio being higher than those obtained from the LB1 endocasts in the present study (Fig. 1). Cerebellar protrusion of LB1 is outside the normocephalic range of 13- to 18-y-old adolescents from the present study (Fig. 1*A*), indicating increased cerebellar length relative to maximal cerebral length in LB1 (adolescent and adult brains are morphologically equivalent; ref. 9). Relative frontal breadth is also outside the normocephalic range, indicating increased cerebral breadth relative to cerebellar width in LB1. A wide cerebrum relative to the cerebellum is consistent with the comment by Falk et al. (8) that LB1 "is ex-

Author contributions: R.C.V. designed research; R.C.V., T.F.B., and R.L.H. performed research; R.C.V. and T.F.B. contributed new reagents/analytic tools; R.C.V. and R.L.H. analyzed data; and R.C.V. and R.L.H. wrote the paper.

The authors declare no conflict of interest.

This article is a PNAS Direct Submission.

[1]To whom correspondence should be addressed. E-mail: rlh2@columbia.edu.

Table 1. MRI-derived craniometric ratios in normocephaly and microcephaly

Sample	Cerebellar protrusion	Relative frontal breadth	Combined ratios
Normo (7)	0.826–0.878	1.167–1.347	1.177–1.248
Micro # 1 (0.1)	**0.963 (>)**	1.273	**1.156 (<)**
Normo (5)	0.844–0.964	1.000–1.400	1.038–1.293
Micro # 2 (0.5)	**0.831 (<)**	1.118	1.161
Normo (6)	0.908–0.941	0.935–1.174	1.018–1.135
Micro # 3 (0.6)	0.908	**0.861 (<)**	**0.981 (<)**
Micro # 4 (0.7)	**0.958 (>)**	0.974	**1.014 (<)**
Normo (7)	0.908–0.941	0.935–1.174	1.018–1.135
Micro #5 (0.8)	**0.894 (<)**	0.974	1.122
Normo (6)	0.877–0.967	0.881–1.214	0.972–1.177
Micro # 6 (1.0)	0.958	0.888	**0.966 (<)**
Micro # 7 (1.1)	0.943	0.883	**0.971 (<)**
Normo (7)	0.880–0.944	0.929–1.047	0.994–1.075
Micro # 8 (1.3)	**0.801 (<)**	1.011	**1.130 (>)**
Normo (6)	0.880–0.926	0.844–1.057	0.975–1.099
Micro # 9 (1.7)	**0.959 (>)**	0.938	0.991
Micro # 10 (1.7)	**0.929 (>)**	1.036	1.056
Normo (6)	0.884–0.926	0.869–1.022	0.989–1.054
Micro # 11 (1.9)	**0.950 (>)**	**1.114 (>)**	**1.084 (>)**
Micro # 12 (1.9)	**0.927 (>)**	**0.785 (<)**	**0.932 (<)**
Normo (6)	0.880–0.959	0.881–0.989	0.972–1.048
Micro # 13 (2.0)	0.911	0.976	1.037
Micro # 14 (2.1)	0.925	1.012 (>)	1.046
Micro # 15 (2.1)	**0.990 (>)**	**1.024 (>)**	1.018
Normo (5)	0.880–0.941	0.881–0.989	0.972–1.048
Micro # 16 (2.3)	**0.971 (>)**	0.976	1.004
Micro # 17 (2.3)	**0.963 (>)**	0.910	0.974
Normo (5)	0.871–0.968	0.905–1.040	0.998–1.047
Micro # 18 (2.6)	0.878	0.968	**1.054 (>)**
Normo (5)	0.873–0.954	0.920–1.010	0.987–1.063
Micro # 19 (5.5)	0.934	**0.878 (<)**	**0.975 (<)**
Normo (5)	0.894–0.942	0.869–1.042	0.976–1.050
Micro # 20 (7.0)	**0.954 (>)**	0.910	0.984
Normo (5)	0.879–0.933	0.869–0.981	0.976–1.060
Micro # 21 (8.5)	**0.961 (>)**	0.906	**0.973 (<)**

Ages in years of the individual microcephalics in parentheses. Age ranges for the controls of the individual microcephalic brains were as follows: # 1–5 (± 1 mo); # 6–18 (± 2 mo); # 19 (± 4 mo); and # 20 and 21 (± 6 mo). Normocephalic values are ranges for the numbers of brains in parentheses. Microcephalic values are individual ratios. Values in bold are outside the range of the control values, either < or >. For the combined ratios, cerebellar protrusion is inverted to allow the ratio to move in the same expected direction. Normo (), normocephalic controls (number of brains); micro, individual microcephalic brains.

tremely brachycephalic," with a cerebral breadth/length ratio exceeding those of fossil and living hominids.

The ratios of the MRI data set were then compared with ratios obtained from six separate measurements (three each) of two LB1 endocasts. These endocasts were obtained from Peter Brown, one of the discoverers of LB1 (for details, see *Methods*). The ratios discriminated LB1 from the normocephalic sample in 5/6 (83%) measurements (Fig. 1*B*). Because the MRI microcephalic cohort consisted of much younger individuals (Table 1) than LB1's estimated adult age, an analysis comparable with that performed for the MRI normocephalic cohort was not accomplished (see below).

The control endocast dataset comprised 79 specimens derived from crania of anatomically modern human (AMH) adults, made by RLH. Initially, these endocasts were compared with the control MRI subset comprising the 24 adolescents ages 13–18 y. All measures of cerebral and cerebellar length and width were similar in the two data sets (Table 2). Relative frontal breadths, when not including the sigmoid sinuses, were nearly identical in the two groups. However, cerebellar protrusion was significantly lower in the MRI sample, despite the similar lengths in the two groups. The discrepancy might relate to the fact that an endocast measurement incorporates both the brain and subarachnoid space, whereas an MRI measurement includes only the brain parenchyma.

The endocast AMH control ratios were then compared with those of 10 microcephalic endocasts (Table 3). Whether the sigmoid sinuses were included or excluded, the ratios were discriminating in 8/10 (80%) of the microcephalic specimens. Combining the two ratios did not improve the discriminatory power. Comparing the ratios in the normocephalic MRI dataset and the microcephalic endocast dataset also showed 80% (8/10) discrimination (sigmoid sinuses excluded). Lastly, the ratios of the endocast microcephalic sample were compared with those of the 24 living microcephalics obtained by MRI (Fig. 2). Cerebellar protrusion ratios in 5/10 (50%) of the microcephalic endocasts were greater than the respective MRI derived ratios, whereas relative frontal breath were equally clustered in the two groups. The reason for the difference in cerebellar protrusion between the two samples presumably relates to the varying ages of the microcephalics, in that the MRI cohort comprised infants and children aged 1 wk to 8.5 y, whereas the endocasts represented both adults and subadults aged 10 y and older. The ratio is slightly lower during infancy, before the cerebellum has undergone its maximal expansion (9). Differences in brain size in the two groups might also account for the difference in cerebellar protrusion. Estimated brain volumes of the MRI microcephalics ranged from 266 to 808 cc, whereas the measured brain volumes of the microcephalic endocasts ranged from 280 to 754 cc. In this regard, brain volume was significantly correlated ($r = -0.64$; $P = 0.046$) with the cerebellar protrusion ratio only in the microcephalic endocasts, indicating that in older individuals the smaller the brain size, the greater the protrusion of the cerebellum.

The ratios of the endocast control dataset were then compared with ratios obtained from the six measurements of the LB1 endocasts (Table 3). The ratios discriminated LB1 from the AMH control sample in 4/6 (67%) measurements (Fig. 3*A*). Comparing LB1 to those of the microcephalic endocast sample, cerebellar protrusion was consistently within the microcephalic range, whereas the LB1 relative frontal breadth was near the upper limit of the microcephalic range, resulting from wider frontal breadths (86 versus 77 mm; $P = 0.02$) combined with more narrow cerebellar widths (86 versus 94 mm; $P = 0.02$) (Fig. 3*B*). The differences suggest extreme brachycephaly and cerebellar hypoplasia in LB1 (8), even compared with known microcephalics.

Finally, the ratios of more distant hominids were compared with those of LB1. The first subset consisted of 17 endocasts derived from fossils of *H. erectus* (brain volumes = 804–1,250 cc). Initially, the ratios were compared with those of the microcephalic endocasts (Fig. 4*A*). Eight of 10 (80%) microcephalic endocasts were outside the range of the *H. erectus* endocasts, owing largely to greater cerebeller protrusion in the microcephalic cohort (means = 0.929 versus 1.01; $P = 0.003$). Similar to the AMH endocasts, the ratios discriminated LB1 from those of *H. erectus* in 5/6 (83%) measurements (Fig. 4*B*). The second subset consisted of four australopithecine endocasts where all four measurements were obtainable. Brain volumes were 427, 450, 530, and 545 cc. The size of the LB1 virtual endocast is estimated at 417 cc (5). Given their similar brain volumes, it was not unexpected that the ratios for LB1 all clustered within the ranges of these early hominids (Fig. 4*C*). Composite graphs derived from linear discriminant function analyses of the two ratios in the AMH, *H. erectus*, australopithecine, and LB1 endocasts are shown in Fig. 5. *H. sapiens* and *H. erectus* cluster together, whereas LB1 clusters with australopithecines and modern microcephalics.

Discussion

In their investigation, Falk et al. (5) found that the combination of the two craniometric ratios, cerebellar protrusion and relative frontal breadth, distinguished 9 microcephalics and 10 normal humans with 100% success. Falk et al. (5) assumed that the cerebellar hemispheres of microcephalics would protrude rela-

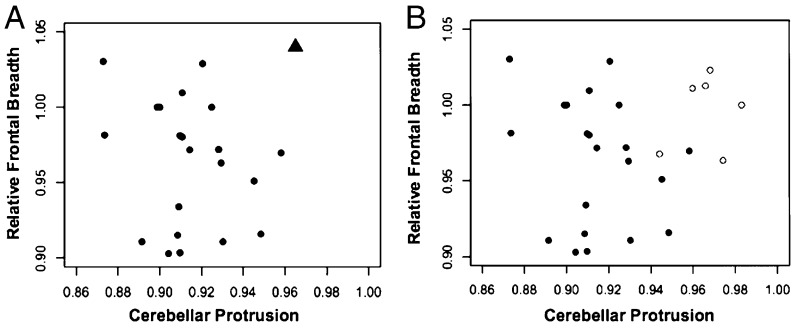

Fig. 1. Scatter plot of relative frontal breadth on cerebellar protrusion from the MRI cohort and LB1. (*A*) Compares MRI-derived ratios in 24 control (normocephalic) adolescents (circles) to those of LB1 (triangle) derived from figure 3 of Falk et al (5). (*B*) Compares derived ratios in 24 control (normocephalic) adolescents (filled circles) to those of LB1 endocasts (open circles).

tively further posteriorly, given the reduced size of the overall brain. Specifically, the ratio that measures the relationship between the length of the brain from the anterior aspect of the cerebral frontal pole to the posterior margin of the cerebellar hemispheres relative to the maximal length of the cerebral hemispheres would be higher in microcephalics. Alternately, relative frontal breadth, which measures the relationship between the width of the cerebral hemispheres and the width of the cerebellum (vermis + hemispheres), would be lower in microcephalics, because the cerebellum would protrude more laterally relative to the cerebral hemispheres.

The present results confirm the discriminating power of the two ratios proposed by Falk et al. (5). Specifically, cerebellar protrusion and relative frontal breadth, measured by MRI, distinguished microcephalic and normocephalic brains in 95% of the cases when used separately or in combination. Also, in the present investigation of 79 normocephalic and 10 microcephalic endocasts, the discriminating power of the two ratios was 80%.

It is not surprising that the ratios derived from the LB1 endocasts cluster with those of *Australopithecus* and those of modern microcephalics. The brain volume of LB1 has been estimated at 417 cc, whereas those of the analyzed australopithecines were 427, 450, 530, and 545 cc. The brain volumes of the microcephalic endocasts were much more variable, ranging from 280 to 754 cc, and there was no relationship between brain size and either ratio in this cohort, presumably the consequence of the diverse nature, severity, and distribution of the brain damage. Despite similar cerebellar volumes relative to cerebral volumes in australopithecines and *H. erectus* (10), the much larger overall brain size of *H. erectus* (804–1,250 cc) was not associated with ratios that overlapped to any significant extent with those of LB1. Thus, very small brain size of whatever etiology can be associated with cerebral/cerebellar dimensions similar to those of LB1.

Table 2. Endocast and MRI measurements and ratios

Measure/ratio	Endocast (n = 79)	MRI (adolescent) (n = 24)	P value
Cerebellar pole—projected	129–170	138–171	0.36
frontal pole, mm	156 ± 9.1	154 ± 5.6	—
Cerebral length, mm	145–187	155–184	0.10
	166 ± 8.9	169 ± 6.9	—
Frontal breadth, mm	89–115	93–111	0.52
	100 ± 6.1	101 ± 4.6	—
Cerebellar width, mm	87–117	98–114	0.13
	105 ± 6.7	106 ± 4.3	—
Cerebellar protrusion	0.768–1.00	0.852–0.958	**<0.001**
	0.939 ± 0.019	0.914 ± 0.026	—
Relative frontal breadth	0.829–1.07	0.881–1.03	0.78
	0.953 ± 0.051	0.956 ± 0.045	—

Values indicate ranges, means, and SDs. Cerebellar widths do not include the sigmoid sinuses. P values by two sample t test; significant differences in bold.

It is unclear as to why the relative frontal breadth ratio of LB1 derived from figure 3 of Falk et al. (5) differs from the ratios of the two endocasts analyzed in the present study. The Falk et al. (5) ratio was obtained from the virtual endocast of a 3D CT reconstruction, whereas the present ratios were derived from one silicon rubber and one plastic endocast provided to RLH by Peter Brown. The relative frontal breadths of these two endocasts were nearly identical (0.99 and 1.00; P = 0.72) and significantly lower than the ratio (1.04) obtained by Falk et al. (5) (P = 0.008). Whatever the reason for the discrepancy, higher frontal breadth ratios in LB1 would increase the discrimination between LB1 and the AMH cohorts obtained from the MRI scans and endocasts. Increased discrimination also would be the case for LB1 versus *H. erectus*.

There is an inherent difficulty with the normative data of Falk et al. (5). Of the 10 normocephalic individuals, two appear to be outliers in reference to relative frontal breadth (1.07 and 1.08). None of the presently reported AMH endocasts even remotely approach these values, the maximum ratio being 0.973 (Table 3). Furthermore, the two values (1.07 and 1.08) are considered outliers by boxplot statistical analysis. The ratios of the entire normocephalic group (n = 10) and the group excluding the outliers (n = 8) are significantly different (P = 0.003), with means of 0.976 and 0.951, respectively. The latter mean is close to the means (0.956 and 0.953) of the same ratio obtained in the present adolescent MRI dataset and AMH endocast datasets, and the ranges are now similar. Removing the two apparent outliers places LB1 outside the range of the Falk et al. (5) normocephalics for relative frontal breadth. For cerebellar protrusion, the Falk et al. (5) and present MRI ratios have similar means (0.928 and 0.914, respectively), with a Falk et al. (5) range of 0.905–0.965. LB1 is at the range limit (0.965) of this ratio. Thus, based solely on the data of Falk et al. (5), the exclusion of LB1 from the microcephalic group is dubious at best.

Qualitative examination of the original LB1 endocast revealed some differences between this specimen and that developed from the 3D CT reconstruction by Falk et al. (5). The original endocast appears to exhibit some pathological features, which include very

Table 3. Endocast normocephalic, microcephalic, and LB1 ratios

Ratio	Normocephalic (n = 79)	Microcephalic (n = 10)	P value	LB1 (n = 6)	P value
Cerebellar	0.768–1.00	0.919–1.11	**0.005**	0.944–0.983	**0.002**
protrusion	0.939 ± 0.019	1.01 ± 0.66	—	0.966 ± 0.013	—
Relative	0.773–0.973	0.814–1.11	0.101	0.963–1.02	**<0.001**
frontal	0.885 ± 0.044	0.934 ± 0.087		0.997 ± 0.025	—
breadth (c)					
Relative	0.829–1.07	0.875–1.18	0.314	1.00–1.24	**0.004**
frontal	0.953 ± 0.51	0.988 ± 1.02	—	1.13 ± 0.09	—
breadth (s)					

The microcephalic and LB1 endocast values represent single measurements by three individuals (D. Broadfield, R.L.H., R.C.V.); shown are ranges, means, and SDs. (c), cerebellar width with sigmoid sinuses; (s), cerebellar width without sigmoid sinuses. P values by two sample t test; significant differences in bold.

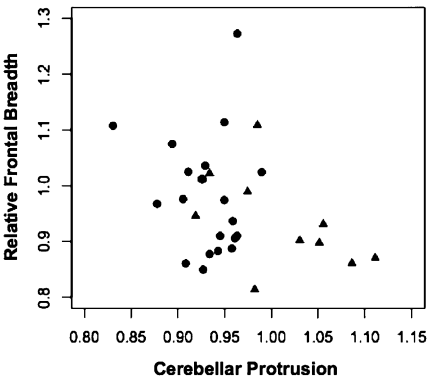

Fig. 2. Scatter plot of relative frontal breadth on cerebellar protrusion in 21 microcephalics from the MRI sample (circles) and in 10 microcephalics from the endocast sample (triangles).

prominent gyri recti of the frontal lobes, suggestive of microgyria; asymmetry of the temporal lobes, the left appearing abnormally small on the lateral surface, the right laterally and inferiorly misaligned; and a keel-like dorsal expansion of the lower brainstem (see also refs. 11 and 12). The left temporal lobe alteration is not apparent on the CT-derived "virtual" endocast.

In conclusion, the LB1 ratios, cerebellar protrusion and relative frontal breadth, both fall outside the range of living normocephalic individuals. The endocast analyses also indicate that the LB1 ratios are just as likely to fall within the range of microcephalic (both primary and secondary) as in the range of normocephalic individuals (Fig. 6). The evidence supports the contention but does not prove that the LB1 endocast represents a pathological microcephalic *H. sapiens* rather than a new species (i.e., *H. floresiensis*). Clearly, more sampling of both modern normocephalic endocasts and those of secondary microcephalics should be accomplished, with an emphasis on more sophisticated morphometric assessments than simple linear measures. The issue of possible pathology will most likely be resolved when further discoveries are made of this hominid.

All other reviewers of the LB1 specimen (directly or indirectly) agree that her brain is exceedingly small (400+ cc), less than one-third the size of AMH's and also well below that of modern pygmies and *H. erectus*. The brain size is most reminiscent of *Australopithecus*. However, the shape and other hallmarks of the endocast, as determined by Falk et al. (5, 7, 8), are consistent with AMH's, whether normal or pathological (4, 12, 13). Physical traits of the cranium, mandible, and dentition have been interpreted as primitive, reminiscent of *Australopithecus* or earlier *Homo* (14–16). Some LB1 bony facial structures are consistent with *H. erectus*, whereas others are consistent with modern humans, including small-bodied individuals (1, 12, 15, 17). In this regard, comparative measurements of the orbits, maxilla, and mandible suggest that the LB1 face is morphologically akin to those of modern local Palauan pygmies (17).

To summarize, the brain of LB1 is australopithecine in size but more modern in configuration, with a disproportionate face. These contrasting features are inconsistent with migration of hominids from Africa to Flores >2 Ma. Ontogenetic studies have shown that facial characteristics at least partially depend on brain size and orientation, (i.e., the larger and more globular the brain, the more retracted the upper part and less prognathic the lower part of the face, owing largely to a change in the basi-cranial angle) (18). In other words, the facial structure is associated with the configuration of the cranial structure. Therefore, if LB1's brain represents that of an ancient hominid, the configuration of its cranial vault should be associated with an equally primitive facial structure akin to *Australopithecus* rather than to *H. erectus* or more recent *Homo* species.

An australopithecine size brain with a more modern configuration also makes little sense unless it is pathological. Increasing encephalization occurs as a consequence of expansion of all lobes of the cerebral hemispheres, especially the frontal and temporal lobes (18). According to Falk et al. (5, 7, 8), LB1 exhibits a relative frontal breadth ratio (frontal breadth/cerebellar width) within or even beyond the range of AMH's, with maximal breadth across the temporal lobes (1). If LB1's brain is evolutionary small and not pathological, its configuration would be expected to be more primitive, akin to *Australopithecus* or *H. erectus*. It is difficult to envision that the brain of the Flores population enlarged adequate to reconfigure its internal cranial structure into modern proportions only later to decrease to its small size while retaining a modern contour.

Other craniofacial as well as postcranial features of LB1 need not represent unique or primitive derived characters. Essentially all of the features assigned to LB1 have been found in more modern humans, especially pygmies, including rudimentary or no chin, megadontia, molar agenesis, and rotated premolars (6, 17). Indeed, most of the features of the LB1 endocast declared as "derived" by Falk et al. (7) are also found in most anthropoids, including hylobatids, as well as in AMHs (19). Many of these characteristics are also seen in extant individuals with pathological microcephaly. Two notable findings in LB1 are the evidence of early suture closure, leading to possible plagiocephaly (20), and weak lower extremity muscle attachments; both features suggest aberrant cranial and limb development (13). Premature closure of the cranial sutures (craniosynostosis) is a hallmark of secondary

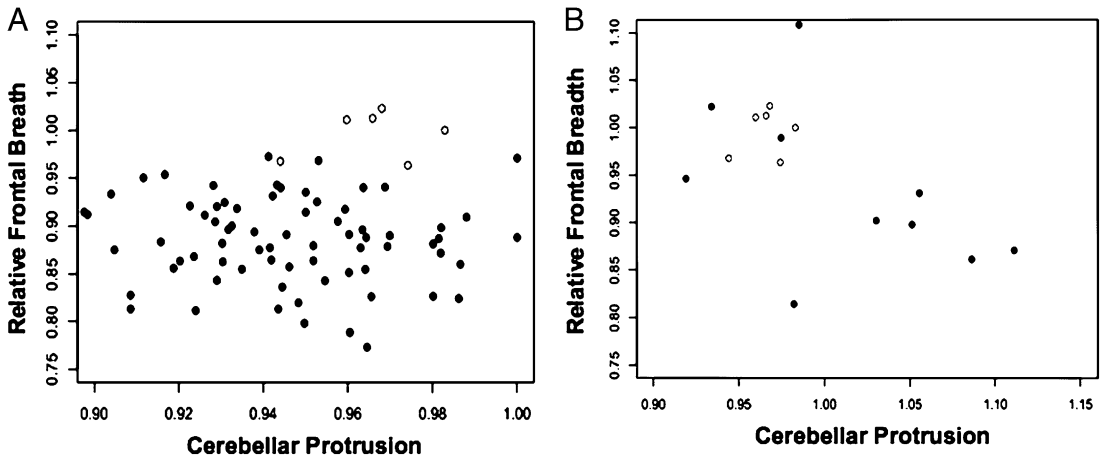

Fig. 3. Scatter plots of relative frontal breadth on cerebellar protrusion from the endocast cohorts. (*A*) compares endocast derived ratios in 79 anatomically modern humans (closed circles) to those of LB1 (open circles); (*B*) compares endocast derived ratios in 10 microcephalics (closed circles) to those of LB1 (open circles).

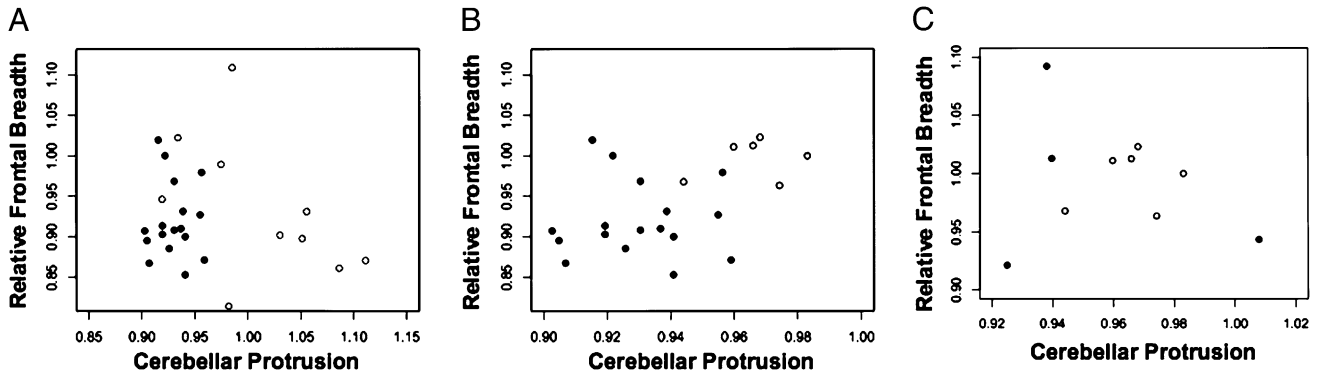

Fig. 4. Scatter plots of relative frontal breadth on cerebellar protrusion from the endocast cohorts. (*A*) Compares derived ratios in 17 *H. erectus* endocasts (filled circles) to those of 10 microcephalic endocasts (open circles). (*B*) Compares derived ratios in 17 *H. erectus* endocasts (filled circles) to those of LB1 (open circles). (*C*) Compares derived ratios in four australopithecines (filled circles) to those of LB1 (open circles).

(acquired) microcephaly, whereas weak muscle attachments are the consequence of lack of mobility, (i.e., paralysis, as seen in severely brain damaged individuals). Muscular paralysis could also account for the curved tibia seen in LB1.

However, in a special issue of the *Journal of Human Evolution* (November 2009), Brown, Morwood, and associates (8, 15, 21–23) addressed many of the issues raised by others regarding the cranio-dental and postcranial features of LB1 and related skeletons, now totaling up to 14 individuals. All of the elements found at the Liang Bua Cave were recently stabilized and hardened, allowing for detailed reexamination and photography. The mandibles as well as multiple bones of the upper and lower extremities were analyzed and found to exhibit a mosaic pattern of both derived (human-like) and primitive morphologies. The investigators opined that the combination of these traits has never been found in either healthy or pathological modern humans (21–23). The limb proportions, like that of the brain, are more akin to *Australopithecus* than to *H. erectus*; whereas the molar teeth, facial height, and degree of prognathism do not follow an australopithecine pattern but rather conform to the *Homo* one. Indeed, the overall morphology of LB1 and her kin combine traits that extend from *Australopithecus* through to modern *H. sapiens*, a truly unique and somewhat confusing pattern not shared by any other extinct or living hominin population (but see ref. 24 for discussion of hypothyroid endemic cretinism in relation to LB1's postcranial bones).

Given the available evidence, it is clearly premature to assign LB1 and associated skeletal finds to a distinct *Homo* species. The existence of a single skull and only a few mandibles provides meager clues as to the type of hominid who inhabited Flores 12–18 kya. There is information to suggest that LB1 was a brain-damaged individual, who suffered secondary microcephaly with associated severe motor disability (cerebral palsy) and likely mental deficiency. No similar specimens have been found to suggest that small-brained and small-bodied hominid populations inhabited Europe or Asia ≈12–18 ka.

The debate regarding the origins of LB1 and her relatives is likely to continue until a major breakthrough occurs (25). The discovery of one of more additional small crania would strongly favor the argument that LB1 represents a newly discovered dis-

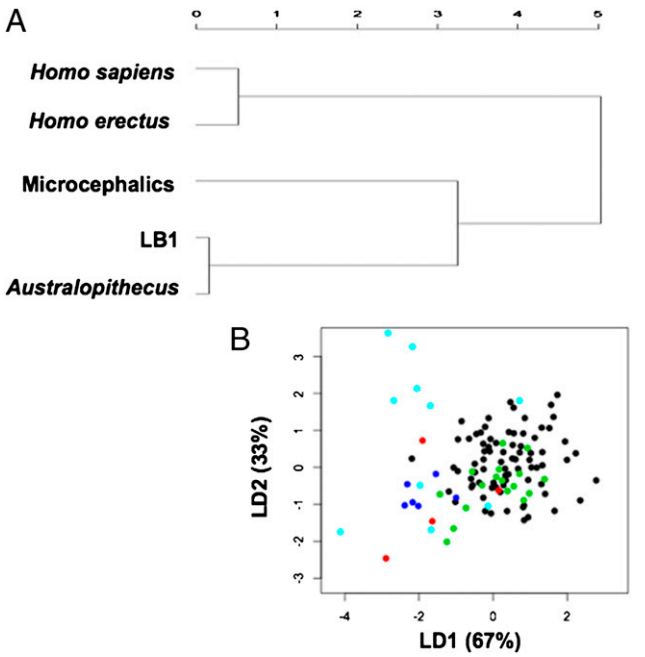

Fig. 5. Composite graphs depicting hominid relationships with LB1 based on cerebellar protrusion and relative frontal breadth ratios. (*A*) Represents an unweighted pair-group method with arithmetic mean (PGMA) distance map of the hominids, including LB1 and modern microcephalics. (*B*) Represents a linear discriminant function analysis of the hominids, including LB1 and modern microcephalics. Black circles represent AMH's (*H. sapiens*), green circles represent *H. erectus*, red circles represent *Australopithecus*, light blue circles represent modern microcephalics, and dark blue circles represent LB1.

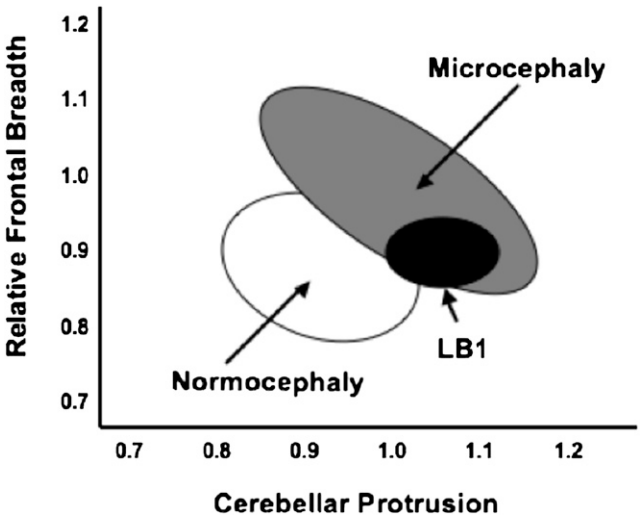

Fig. 6. Venn diagram of endocast normocephlic, microcephalic, and LB1 ratios. LB1 overlaps primarily with the microcephalic specimens. Data derived from Figs. 3 and 4.

tinct *Homo* species. More comparative 3D morphometric assessments of existing specimens using available techniques rather than the use of simple linear ratios also would be worthwhile (15). Even more enlightening would be a DNA analysis of available skeletal specimens to determine the true genetic origin of the Flores population under consideration. The wide genetic variation of anatomically modern humans would be readily distinguished from the more limited diversity of an isolated, ancestral population that inhabited Flores 1 or more Ma.

Methods

The sampled MRI population included patients evaluated by WellSpan Neuroscience. The normocephalic cohort comprised 118 patients, each of whom had undergone a brain MRI and whose scan was interpreted as "normal" by a WellSpan Health radiologist (9). Ages of the patients ranged from 1 postnatal week to 18.5 y, including 55 females and 63 males (9). The second cohort included 21 infants and children with a diagnosis of microcephaly (occipito-frontal circumference < second percentile for age) and an associated MRI scan. Based on clinical and radiographic information, the microcephalic individuals were classified as primary (genetic defect, chromosomal anomaly, syndrome, sporadic developmental anomaly, familial microcephaly) (n = 11), secondary (acquired intrauterine insult) (n = 4), or unknown cause (n = 6). The MRI research plan was approved by the WellSpan Health Institutional Review Board on July 6, 2009. All MRI examinations were performed as previously described (9).

Four specific craniometric measurements were obtained from MRI images in the sagittal and axial planes (9). These measures were the same as those obtained by Falk et al. (5) and included (*i*) cerebral length, (*ii*) cerebellar pole to projected frontal pole, (*iii*) frontal breadth (at anterior temporal pole), and (*iv*) cerebellar width. Because the sigmoid sinuses are not visualized on MRI, these structures were not included in the measurement of cerebellar width (see below). Two ratios were then determined; specifically cerebellar protrusion (2/1) and relative frontal breadth (3/4). The measures of these two ratios also were extracted from figure 3 of Falk et al. (5). Brain volume of the MRI microcephalic data set was determined by a described technique, using linear measures in length, width, and height (9).

The endocast data set comprised 79 normocephalic specimens prepared by RLH that represented anatomically modern human adult crania from a variety of sources, including the American Museum of Natural History (26). Detailed information regarding the specimens, reconstruction, and anatomical references has been published (27). Eight microcephalic endocasts were provided to R.L.H. by Milford Wolpoff and the AMNH. At least two of these endocasts (96-11-128A and AMNH2792a) were the same as those reported by Falk et al. (5, 8), one of which was a subadult at 10 y of age. D. Grimaud-Herve provided the endocast of N. Ferry, a nannocephalic, and R.D. Martin and S. MacLarnon provided an endocast of a microcephalic from India, housed at the RCS. The 17 *H. erectus* endocasts were the same as those reported by Bruner and Holloway (26). Four australopithecine endocasts also were available in which all four linear measures could be determined. These endocasts included BOU-VP-12/130, SK1585, Konso, and Omo-L338Y. Two LB1 endocasts were provided to R.L.H. by Peter Brown, the first derived from a stereolith of the original cranium, and the second derived from a 3D, computed tomographic reconstruction or virtual endocast that had undergone smoothing processes (5). The same four craniometric measures as described for the MRI images were obtained from all of the endocasts, using spreading and sliding calipers. Cerebellar lengths were made directly on the endocasts by measuring the distance between the frontal pole and the most posterior aspect of the cerebellum, usually on the right side. Cerebellar widths included and excluded the sigmoid sinuses.

Data analysis included a statistical comparison of MRI and endocast measurements and ratios between normal and microcephalic brains within specific age categories as dictated by the ages of the microcephalic infants and children. Statistical methods included two-sample, unpaired, two-tailed t test, linear correlation, and linear discriminant function analysis. The sigmoid sinuses were excluded when intragroup MRI data or intergroup MRI and endocast data were compared. The sigmoid sinuses were included when intragroup endocast data were compared, as was the case with the Falk et al. (5, 8) analyses. All statistical analyses were performed, and graphics were produced by using "R" software (28).

ACKNOWLEDGMENTS. We thank Douglas Broadfield for assisting in the measurements of the microcephalic and LB1 endocasts; Desiree Lerro for assisting in the MRI measurements; and Tim White for reviewing the manuscript and providing helpful suggestions.

1. Brown P, et al. (2004) A new small-bodied hominin from the Late Pleistocene of Flores, Indonesia. *Nature* 431:1055–1061.
2. Morwood MJ, et al. (2004) Archaeology and age of a new hominin from Flores in eastern Indonesia. *Nature* 431:1087–1091.
3. Morwood MJ, et al. (2005) Further evidence for small-bodied hominins from the Late Pleistocene of Flores, Indonesia. *Nature* 437:1012–1017.
4. Martin RD, Maclarnon AM, Phillips JL, Dobyns WB (2006) Flores hominid: New species or microcephalic dwarf? *Anat Rec A Discov Mol Cell Evol Biol* 288:1123–1145.
5. Falk D, et al. (2007) Brain shape in human microcephalics and *Homo floresiensis*. *Proc Natl Acad Sci USA* 104:2513–2518.
6. Richards GD (2006) Genetic, physiologic and ecogeographic factors contributing to variation in *Homo sapiens: Homo floresiensis* reconsidered. *J Evol Biol* 19: 1744–1767.
7. Falk D, et al. (2005) The brain of LB1, *Homo floresiensis*. *Science* 308:242–245.
8. Falk D, et al. (2009) LB1's virtual endocast, microcephaly, and hominin brain evolution. *J Hum Evol* 57:597–607.
9. Vannucci RC, Barron TF, Lerro D, Antón SC, Vannucci SJ (2011) Craniometric measures during development using MRI. *Neuroimage* 56:1855–1864.
10. Weaver AH (2005) Reciprocal evolution of the cerebellum and neocortex in fossil humans. *Proc Natl Acad Sci USA* 102:3576–3580.
11. Weber J, Czarnetzki A, Pusch CM (2005) Comment on "The brain of LB1, *Homo floresiensis*". *Science* 310:236–237, author reply 236.
12. Henneberg M, Thorne A (2004) Flores may be pathological *Homo sapiens*. *Before Farming* 1:2–4.
13. Jacob T, et al. (2006) Pygmoid Australomelanesian *Homo sapiens* skeletal remains from Liang Bua, Flores: Population affinities and pathological abnormalities. *Proc Natl Acad Sci USA* 103:13421–13426.
14. Argue D, Donlon D, Groves C, Wright R (2006) *Homo floresiensis:* Microcephalic, pygmoid, Australopithecus, or Homo? *J Hum Evol* 51:360–374.
15. Baab KL, McNulty KP (2009) Size, shape, and asymmetry in fossil hominins: The status of the LB1 cranium based on 3D morphometric analyses. *J Hum Evol* 57: 608–622.
16. Gordon AD, Nevell L, Wood B (2008) The *Homo floresiensis* cranium (LB1): Size, scaling, and early Homo affinities. *Proc Natl Acad Sci USA* 105:4650–4655.
17. Berger LR, Churchill SE, Klerk SE, Quinn RL (2008) Small-bodied humans from Palau, Micronesia. *PLoS ONE* 3:e1780.
18. Lieberman DE, McBratney BM, Krovitz G (2002) The evolution and development of cranial form in *Homo sapiens*. *Proc Natl Acad Sci USA* 99:1134–1139.
19. Holloway RL, Schoenemann T, Monge J (2010) The hobbit brain: Some doubts about its "derived features". *Am J Phys Anthropol* 141(S50):130.
20. Kaifu Y, et al. (2009) Brief communication: "Pathological" deformation in the skull of LB1, the type specimen of *Homo floresiensis*. *Am J Phys Anthropol* 140: 177–185.
21. Brown P, Maeda T (2009) Liang Bua *Homo floresiensis* mandibles and mandibular teeth: A contribution to the comparative morphology of a new hominin species. *J Hum Evol* 57:571–596.
22. Jungers WL, et al. (2009) Descriptions of the lower limb skeleton of *Homo floresiensis*. *J Hum Evol* 57:538–554.
23. Larson SG, et al. (2009) Descriptions of the upper limb skeleton of *Homo floresiensis*. *J Hum Evol* 57:555–570.
24. Oxnard C, Obendorf PJ, Kefford BJ (2010) Post-cranial skeletons of hypothyroid cretins show a similar anatomical mosaic as *Homo floresiensis*. *PLoS ONE* 5:e13018.
25. Aiello L.C. (2010) Five years of *Homo floresiensis*. *Am J Phy Anthropol* 142:167–179.
26. Bruner E, Holloway RL (2010) A bivariate approach to the widening of the frontal lobes in the genus Homo. *J Hum Evol* 58:138–146.
27. Holloway RL, Broadfield DC, Yuan MS (2004) Brain endocasts: The paleoneurological evidence. *The Human Fossil Record*, Vol III, (Wiley, Hoboken, NJ).
28. R Development Core Team (2009) R: A language and environment for statistical computing. *The R Foundation for Statistical Computing*, Vienna. Available at http://www.R-project.org.